THE SIMPLE EVALUATION METHOD OF SHEAR STRESS GENERATED BY EARTHQUAKE IN SOIL GROUND

Tsuneo IMAI, Keiji TONOUCHI and Takashi KANEMORI

Abstract

Accurate evaluation of shear stress and the ability to forecast amplitude of acceleration, velocity and displacement of seismic waves generated by earthquakes are essential factors in aseismic design planning as well as in the assesment of the liquefaction potential of sandy ground. A simple method proposed by Seed forecasts shear stress generated by earthquakes. In Seed's method, a column of soil in the ground is arbitrarily taken as a unit for the basis of calculations. In order to approximate actual shear stress in relation to base shear of this column, which is treated as a rigid body, a correction coefficient (or, as Seed calls it, a "stress reduction" coefficient) r_d is used. Besides Seed, this coefficient has also been proposed by Iwasaki, et al. However, little investigation of the reliability of this coefficient has been carried out.

In this paper, the results of many response analyses have been used to examine to correction coefficient r_d from a number of angles. On the basis of this investigation, the authors proposed a simple evaluation method which uses "time-related" r_d distribution values in place of the heretofore used "depth-related" values. Using this method, the authors have forecast shear stress that would be generated during earthquakes. They have found that the results given by this method are similar to those yielded by detailed response analyses.

1 INTRODUCTION

Much past experience has made it very clear that there is a close relationship between earthquake damage and the type of ground in which the earthquake occurs. This is to say that the behavior of the ground during an earthquake varies according to the type of ground. In this regard, in order to prevent or at least minimize damage due to earthquakes, careful consideration of the probable behavior of the ground during earthquakes is essential. Various types of ground behavior forecasting methods have become available.

Methods for predicting ground behavior include the wave amplitude of acceleration, velocity and displacement. In addition, the evaluation of shear stress generated during earthquakes is important for planning aseismic design of structures as well as for assessment of liquefaction potential of sandy ground.

Generally, response analysis is used to assess various types of wave amplitude or shear stress data. Assessment techniques include the Lumped Mass Method, a method based on wave motion theory and the Finite Element Method. However, as an alternative to these complex methods that is frequently used, the method proposed by Seed (1971)[1] is a simple way of forecasting shear stress generated during earthquakes.

In Seed's method, surface acceleration and overburden pressure are used to calculate

shear stress at various depths. In this method, a column of soil, regarded as a rigid body, is taken as a unit. In order to approximate actual shear stress in relation to base shear below this column, a correction coefficient is used. The method of calculation is relatively simple. Thus, this method is commonly used when substantial areas of ground are to be investigated or simply when a general idea of shear stress is all that is needed.

In Seed's method for evaluating shear stress, the correction coefficient r_d is used to produce results that more closely approximate actual shear stress. While this coefficient has been proposed by Iwasaki (1978)[2] as well as Seed, actually little investigation of the reliability of this coefficient has been carried out. The fact is that frequently the r_d value that has been proposed does not agree with values that have been calculated on the basis of shear stress values obtained by response analysis.

Thus, the authors have taken up the problem of the value of r_d[3),4)]. The results of many response analyses have been used to examine the correction coefficient from a number of aspects. On the basis of this investigation, we propose a simple evaluation method. Using this method, we have evaluated shear stress generated during earthquakes and compared our results with the results of other methods. This paper is a report on these results.

2 THE SIMPLIFIED METHOD

Below is a description of the method proposed by Seed for evaluating shear stress at the time of an earthquake.

As shown in Figure 1, the ground is considered to be made up units of soil column of specified areas. Assuming that each soil column is a rigid body, Formula (1) expresses base shear τ at the bottom of the column when subjected to acceleration a.

$$\tau = \frac{a}{g}\sigma_v \tag{1}$$

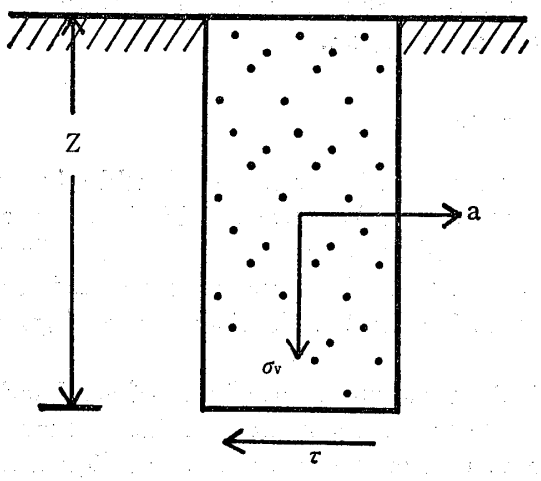

Fig. 1 Shear strain on the unit soil column

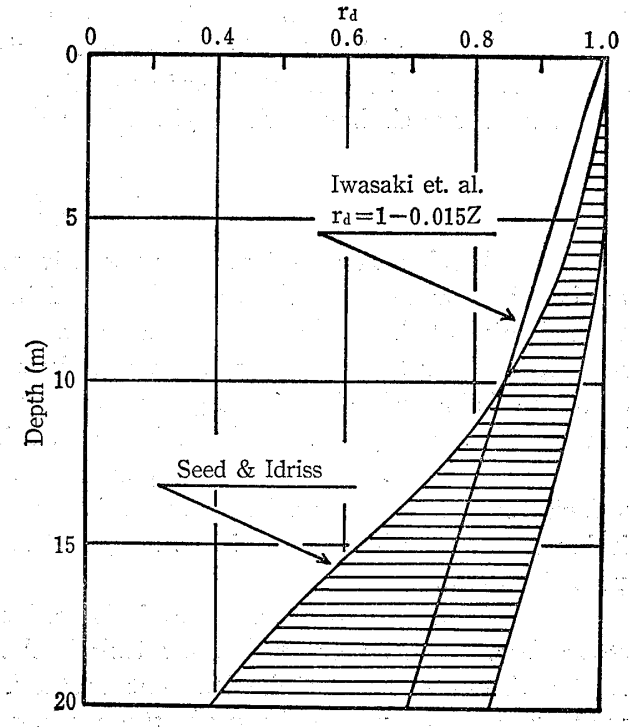

Fig. 2 r_d distribution (old proposal)

where, σ_v=overburden pressure at the base of soil column (i.e., weight of the column)
and g=acceleration of gravity.

However, in actuality, the soil column is not a rigid body, but an elastic body that undergoes deformation. Consequently, if we designate r_d as a quantity to correct for this, shear stress during earthquakes τ_d may be expressed as the following formula:

$$\tau_d = \tau \cdot r_d \tag{2}$$

Seed refers to r_d as a "stress reduction coefficient". Thus, it can be said that r_d is a correction factor for making τ approximately equal to τ_d, and in this way, signifies a departure from the rigid body concept.

Figure 2 shows the distribution of r_d proposed by Seed and Iwasaki for different depths. Using the results of response analysis of a number of ground models of sand layers located within 15 meters from the surface, Seed found the distribution of r_d values shown by the crosshatching in the figure. Iwasaki et al. carried out a series of response analysis tests of 6 different kinds of input waves in different ground models. Different values for r_d were found for each input wave. In addition, it was found that the value of r_d falls off as depth increases according to a certain proportion, and that this proportion is greater the shorter the predominant period of the input wave. However, for practical purposes, they took the mean value from their results to propose a value for r_d as $1-0.015 \cdot z$, where z=depth. This method of expressing

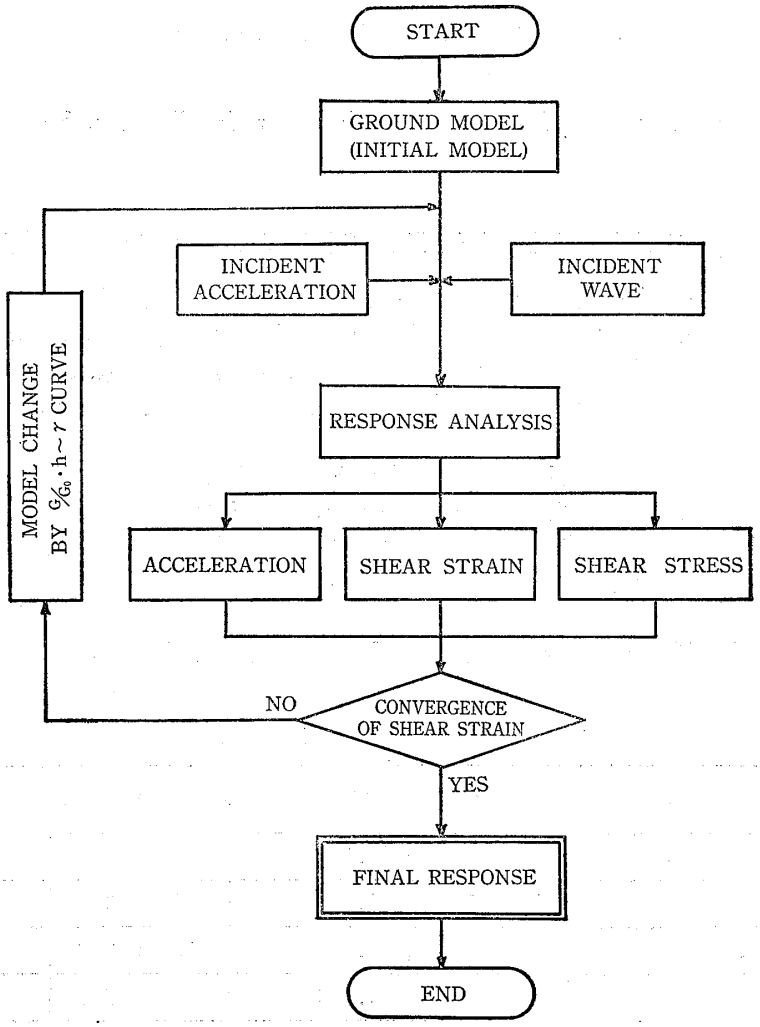

Fig. 3 Response analysis method outline

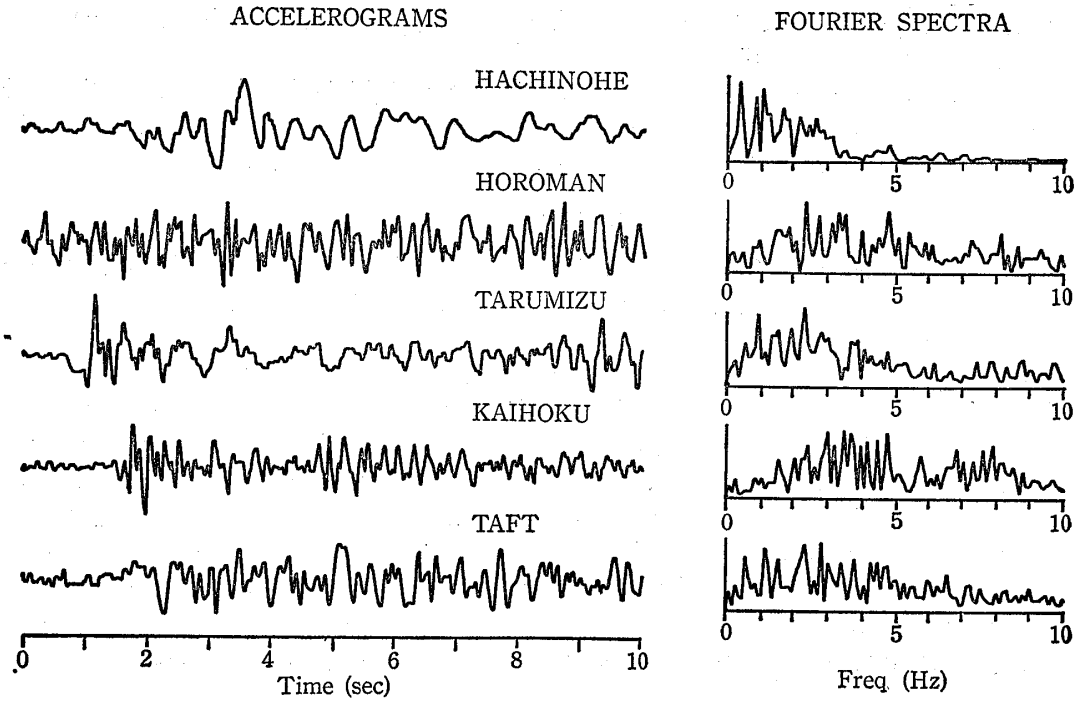

Fig. 4 Input waveforms for response analysis

r_d is used in the government publication, "Specifications for the Earthquake-Resistant Design of Highway Bridges"

3 METHODS OF INVESTIGATION CORRECTION COEFFICIENT r_d

This report is based on numerous response analyses carried out by the authors. The response analysis method used is based on multiple reflection theory[5] for S waves in horizontally layered ground. The method takes into account the non-linearity (i.e. strain dependency) of dynamic deformation characteristics of the soil. Figure 3 is a diagramatic representation of the process of response analysis.

Response analysis was carried out on the 5 waveforms shown in Figure 4 for a total of 143 calculations. Table 1 shows the essential data concerning each of the 5 types of waves used[6)~9)]. Material published by California Institute of Technology, the Ministry of Construction's Public Works Research Institute and the Ministry of Transport's Port and Harbor Research Institute provided this data.

In order to classify the different types of ground in which response analysis was carried

Tabel 1 Essential data on input waves used in the investigation

Name	Date	Focal region	M	Depth (km)	△ (km)	Comp.	Max. acc. (gal)	Notes
HACHINOHE	May 16, 1968	Off Tokachi	7.9	0	186	NS	233	P.H.R.I.
HOROMAN	May 16, 1968	Off Tokachi	7.9	0	154	TR	52	P.W.R.I.
TARUMIZU	June 12, 1978	Off Miyagi Pref.	7.4	40	120	TR	177	P.W.R.I.
KAIHOKU	June 12, 1978	Off Miyagi Pref.	7.4	40	90	LG	193	P.W.R.I.
TAFT	July 21, 1952	Central Carifornia	7.7	0	44	S69E	158	E.E.R.L.

out, the following formula for calculating f_0, a value which corresponds to predominant frequency of the ground was used.

$$f_0=\left(4\sum_{i=1}^{n-1}\frac{H_i}{V_i}\right)^{-1}$$

where, V_i=S wave velocity of ith layer
H_i=thickness of ith layer
n=number of layers of the ground model

Figure 5 shows the distribution of f_0 values for each type of seismic wave. As shown in the figure, many of the grounds for which response analysis was carried out has a predominant frequency of below 1 Hz, ("Ground Type 4", as described in "Specifications for the Earthquake-Resistant Design of Highway Bridges").

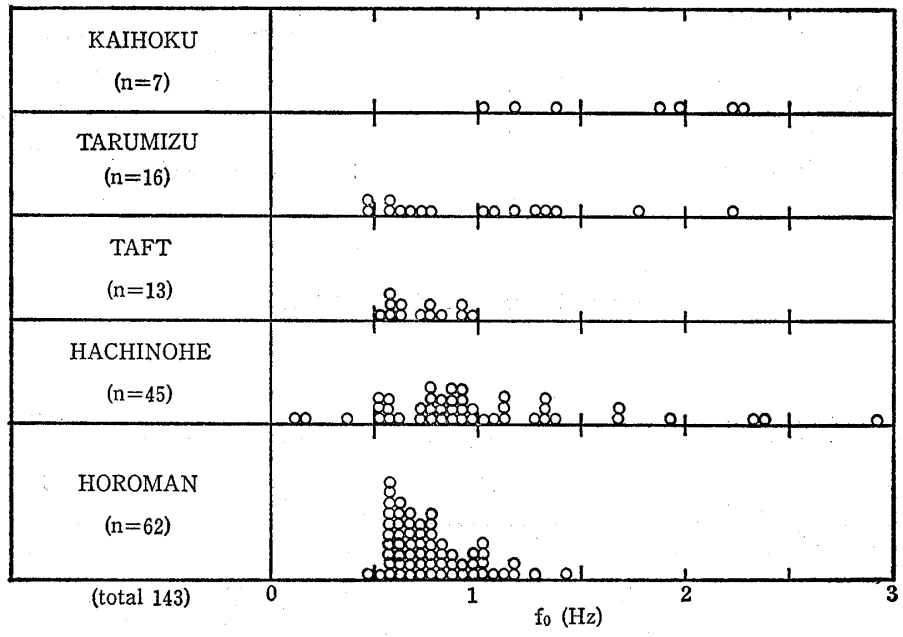

Fig. 5 Distribution of predominant frequencies in response analysis ground models

4 DEPTH-RELATED r_d DISTRIBUTION (OLD METHOD)

4.1 Range of Depth-Related r_d Distribution

Heretofore, correction coefficient r_d has been expressed according to its distribution in relation to depth (in this paper, this method of expressing r_d is referred to as "depth-related r_d distribution"). Both Seed and Iwasaki have made proposals for expression of r_d distribution in this way.

Figure 6 (a) shows distribution of r_d values plotted against depth. The data is the result of the 143 response analyses carried out by the authors. Figure 6 (b) is the previously shown graph of r_d distribution based on findings by Seed and Iwasaki, shown once again for purposes of comparison. It can be clearly seen that the distribution of values for r_d in Figure 6 (a) simply does not fit within what had previously been accepted as the range of r_d values. This figure illustrates that r_d is not an invariable value for a given depth, but is greatly influenced by conditions related to type of input waves, ground conditions, etc.

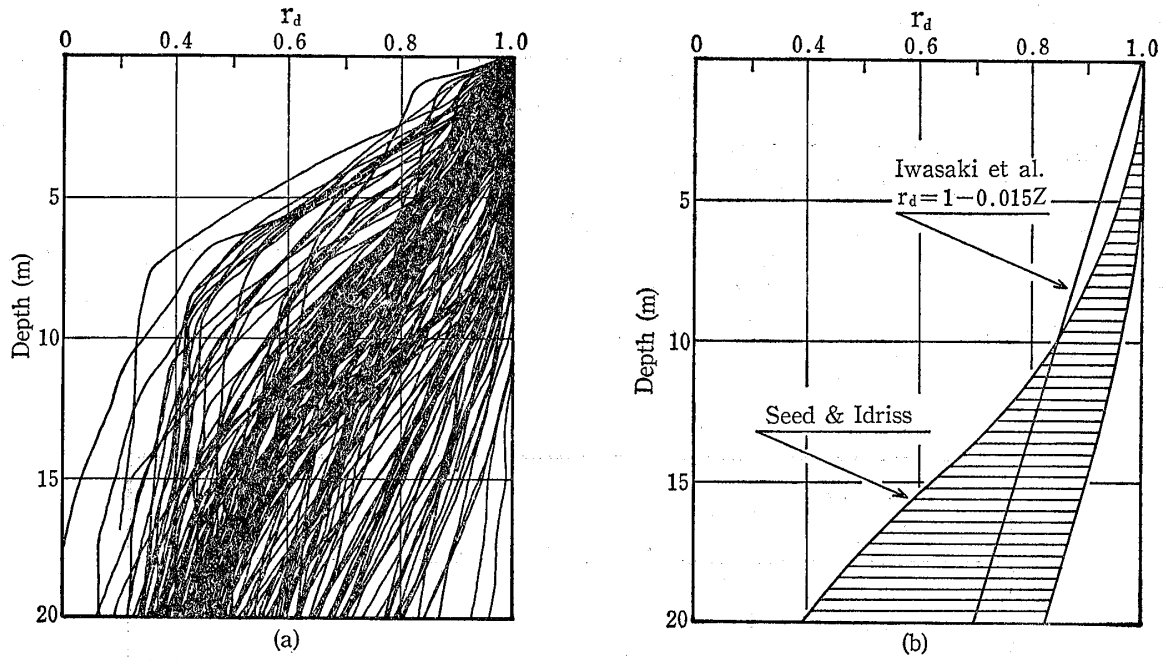

Fig. 6 Depth-related r_d distribution

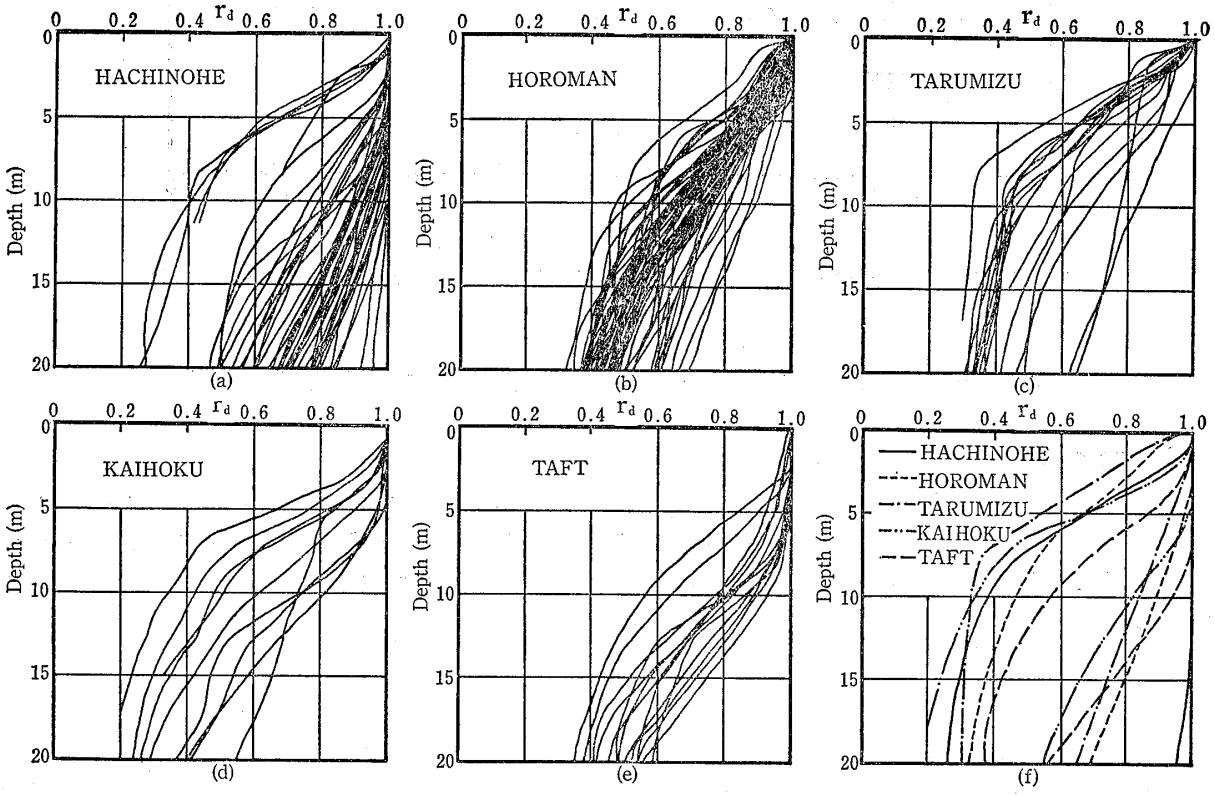

Fig. 7 Depth-related r_d distribution arranged accordings to type of input wave

4.2 Differences in r_d Distribution due to Type of Input Wave

Figure 7 is a breakdown of the r_d curves shown in Figure 6, arranged according to the 5 different stations at which the seismic waves were monitored. It can be seen from these graphs that r_d values vary according to the seismic wave. With the HACHINOHE waves, r_d does not decrease very much with increases in depth. However, with the TARUMIZU waves, r_d falls off drastically over an interval of 10 meters from the surface. With the HOROMAN waves, r_d generally decreases linerally with increasing depth. The TAFT waves appear to be midway in tendency between the HOROMAN and HACHINOHE waves. Thus, while it is clear that r_d distribution tends to extend over a considerable range even for a single type of waveform, it is just as clear that input wave alone is not the only factor that determines r_d value.

4.3 Differences of r_d Distribution due to Ground Condition

Because the distribution of response acceleration values according to depth reflects ground conditions, we can probably state with confidence that there must be some correlation between acceleration and r_d distribution.

The authors have taken 5 representative r_d curves from their response analyses of HACHINOHE waves that show a relatively wide distribution of r_d values. Using this data, the relationship between r_d distribution and distribution of response acceleration values were plotted. The results are shown in Figure 8(a), 8(b) and 8(c). Figure 8(a) and 8(b) plot acceleration values against depth, with acceleration values in (a) normalized in relation to the base layer, while acceleration values in (b) normalized in relation to the surface. Figure 8(c) plots distribution of r_d values against depth. It can be seen from these figures that the proportion by which r_d values decrease according to depth shows a relatively good correlation between normalized acceleration values at the surface and distribution of acceleration values. However, normalized base acceleration values do not show any particular correlation at all. From this, we may infer that r_d distribution is not greatly influenced by all layers above the base layer, but rather is largely determined by ground conditions in shallow layers only.

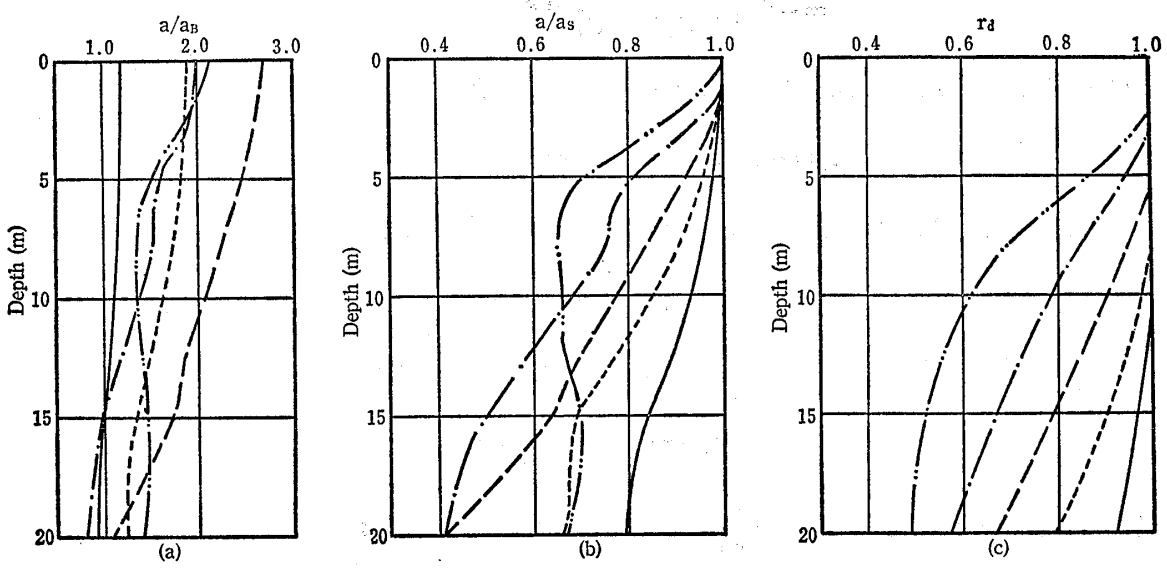

Fig. 8 Comparison of r_d distribution and acceleration distribution

5 TIME RELATED r_d DISTRIBUTION (PROPOSED METHOD)

5.1 r_d as derived from Wave Motion Theory

Seed's simplified method is based on the concept of a balance of forces within a hypothetical soil column. In this section, however, we will consider r_d from the standpoint of wave motion theory.

As shown in Figure 9, a semi-infinite medium in which S wave velocity is uniform is hypothisized. Let us suppose that we have an incident wave with angular frequency ω and displacement amplitude v_o. If we designate the time in which this wave arrives at the surface as t, surface displacement v_s is

$$v_s=2v_o e^{i\omega t}$$

and acceleration a_s is

$$a_s=-2\omega^2 v_o e^{i\omega t} \tag{3}$$

Also, at a given depth z, displacement v_z is expressed by the following formula which combines upward and downward waves:

$$v_z=v_o e^{i\omega\left(t-\frac{z}{V_s}\right)}+v_o e^{i\omega\left(t+\frac{z}{V_s}\right)}$$

$$=v_o\left(e^{i\omega\frac{z}{V_s}}+e^{-i\omega\frac{z}{V_s}}\right)e^{i\omega t}$$

where V_s=S wave velocity.

Consequently, shear stress τ_z at depth z is expressed by the following formula:

$$\tau_z=G\frac{\partial v_z}{\partial z}$$

$$=iG\frac{\omega}{V_s}\left(e^{i\omega\frac{z}{V_s}}-e^{-i\omega\frac{z}{V_s}}\right)e^{i\omega t}$$

$$=-2v_oG\frac{\omega}{V_s}\sin\frac{\omega z}{V_s}e^{i\omega t}$$

Here, G is rigidity. Thus, from the relationship $G=\rho V_s^2$

$$\tau_z=-2v_o\rho V_s\omega\sin\frac{\omega z}{V_s}e^{i\omega t} \tag{4}$$

Starting with the following formula which defines r_d,

$$r_d=\frac{(\tau_z)_{\max}}{(a_s)_{\max}\sigma_v} \tag{5}$$

by substituting Formulas (3) and (4) into Formula (5), we get

$$r_d=\frac{V_s}{\omega z}\sin\frac{\omega z}{V_s}$$

and if we use the expression $T=\frac{z}{V_s}$, we obtain the following:

$$r_d=\frac{1}{\omega T}\sin(\omega T) \tag{6}$$

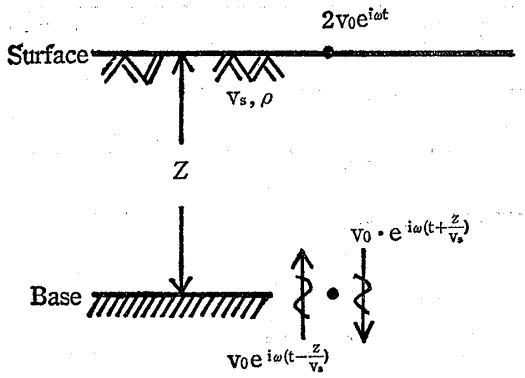

Fig. 9 Propagation of seismic waves

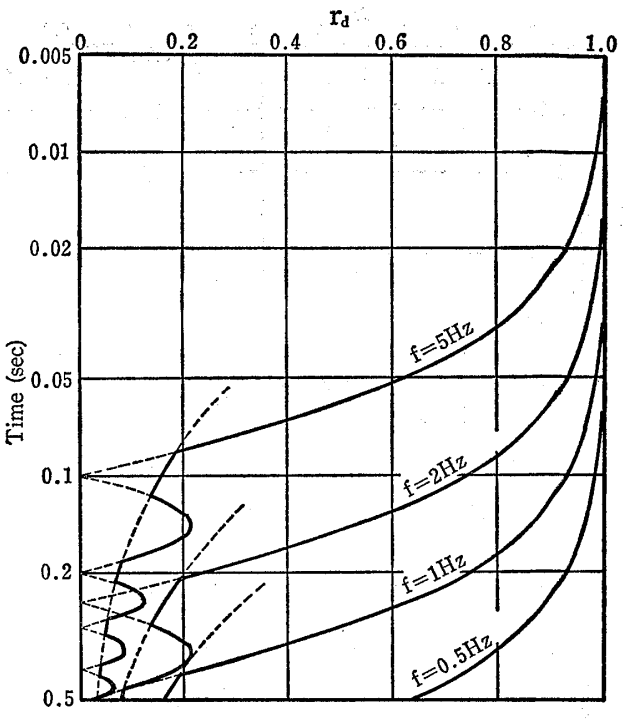

Fig. 10 Theoretical r_d distribution in semi-infinite media

When Formula (6) is applied to stationary waves, in the time before the downward wave reflected by the surface has not reached the point, $\left(T<\frac{z}{V_s}\right)$, because only the upward wave need be concidered, by eliminating the expression for the downward wave, we get

$$r_d=\frac{1}{2\omega T} \tag{7}$$

Thus, in a semi-infinite elastic homogenous medium, r_d is expressed either by Formula (6) or (7), whichever is the larger value. Figure 10 shows calculated r_d values for a semi-infinite elastic homogenous medium for frequencies of 0.5, 1, 2 and 5 Hz.

The above has shown that the correction coefficient r_d is a function of frequency of incidental waves as well as T, arrival time of S waves from the surface to a depth z. (Hereafter travel time is given as T.)

5.2 Actual Time-Related r_d Distribution Values

It was shown in the last section that in a semi-infinite elastic medium, r_d is represented as a function of the frequency elements of input waves and travel time of S waves. When we consider this, if we were to consider r_d in relation to travel time for each input wave, even in the average multilayered ground it can be expected that rather than depth related r_d distribution, r_d distributed arranged according to travel time of each input wave would produce a tighter distribution pattern.

Figure 11 is the r_d distribution arranged according to travel time of each wave using the same depth-related r_d distribution data as in Figure 6. In this paper, this type of arrangement will be referred to as time-related r_d distribution. Now, if we compare the time-related r_d distribution in Figure 11 to depth-related r_d distribution in Figure 6, we find that the former shows the

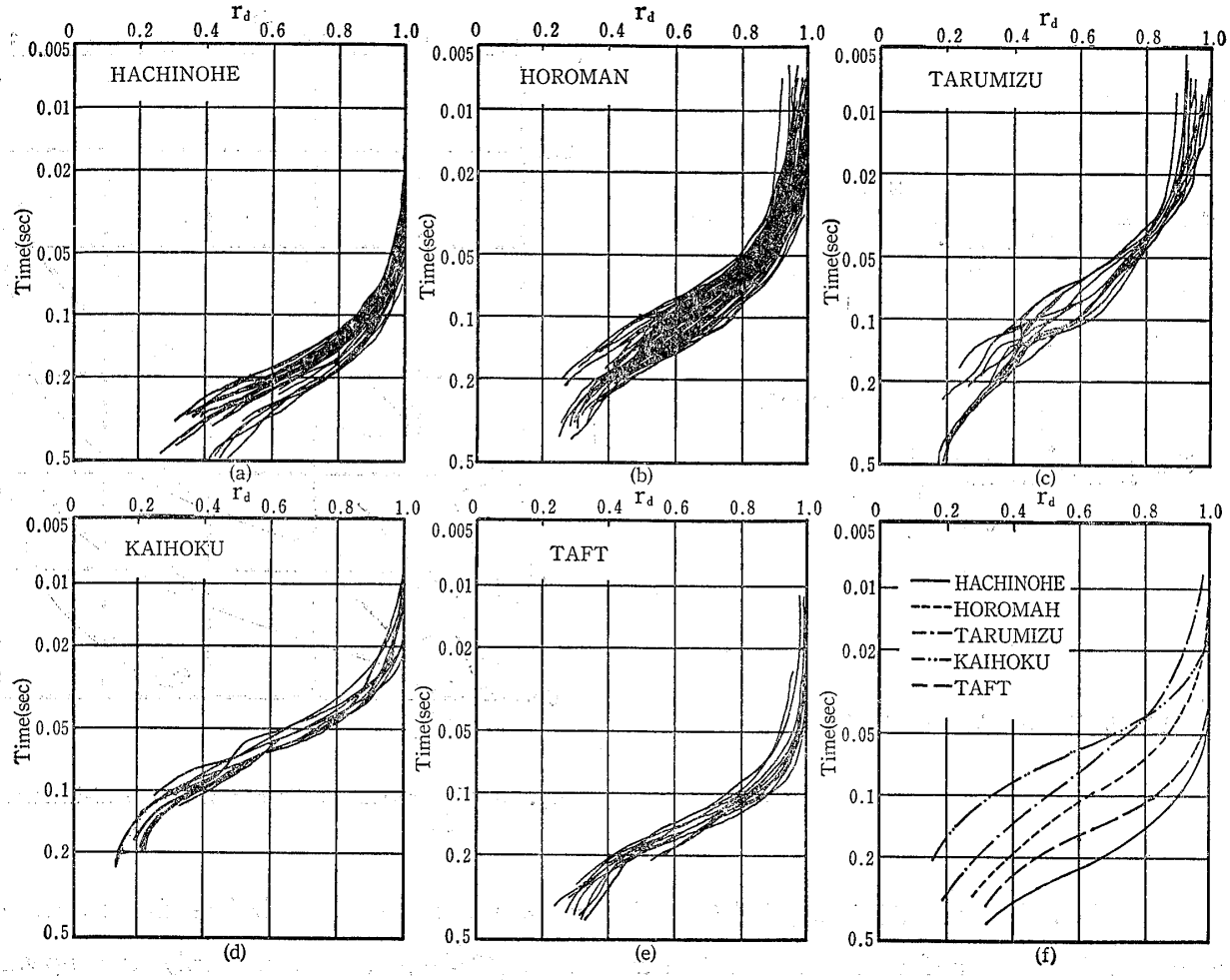

Fig. 11 Time-related r_d distribution

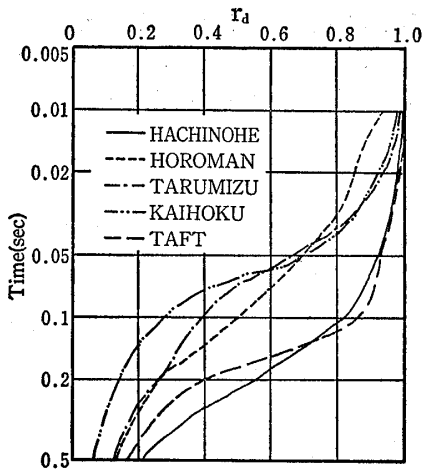

Fig. 12 Actual r_d distribution in semi-infinite media

better concentration. Figure 11(f) is a comparison of the mean values of r_d distribution for each input wave form. Because r_d values reflect frequency characteristics of input waves, a different distribution curve for each wave is obtained.

In the above, we have seen that if r_d distribution in multilayered ground is expressed in relation to travel time, regardless of ground conditions, there is a tendency for similar distribution curves to be described for each input wave.

Next, we have calculated r_d values for 5 input waves in a semi-infinite elastic medium. This is shown in Figure 12. If we compare this figure and the single frequency r_d values of Figure 10, we can see that although there is a relatively similar distribution pattern, but the factor of single frequency r_d values alone is not sufficient to account for all travel times. That is to say, general input wave form r_d values are made up of many different types of frequency elements. Also, if we compare with response analysis results (Figure 11) we see that the r_d distribution in Figure 10 generally corresponds to the lower limit (small r_d values) of r_d distribution in Figure 11.

5.3 r_d Distribution in a Ground Model

Having achieved the satisfactory results described above, the authors carried out response analysis on a simplified two-layer ground model to consider the effects of ground conditions on r_d distribution.

In two-layer ground models, response properties are determined by three parameters: (1) impedance ratio α; (2) travel time from base layer to surface T_o; and (3) damping factor of the ground. Here, $\alpha = \frac{\rho_1 V_1}{\rho_2 V_2}$ (where ρ=density, V=S wave velocity, 1=surface layer and 2=base layer). $T_o = d/V$ (where d=thickness of surface layer). When T_o is increased by a factor of 4, it corresponds to the primary predominant frequecy of the ground. The authors have investigated the influence on r_d distribution of the effects of changing each of these three parameters. Below, representative examples are given of HACHINOHE input waves, with their relatively long predominant element and HOROMAN input waves, which include many short period elements.

Figure 13 is an investigation of the effects of impedance ratio α. The changes in r_d distribution when α=1.0, 0.5 and 0.2 are shown. It can be seen that there is little change in r_d distribution with changes in impedance ratio. Next, we investigated the results when T_o=0.1, 0.2 and 0.5. This is shown in Figure 14. In this case, some changes in r_d distribution for HOROMAN

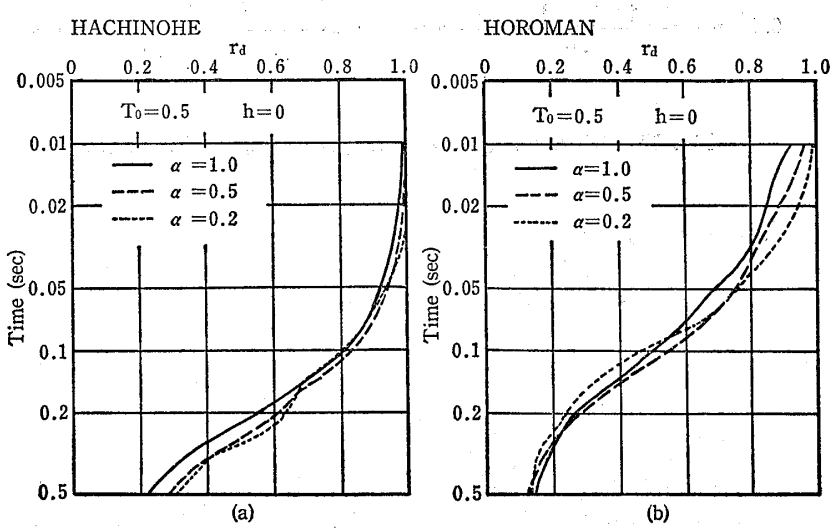

Fig. 13 Effect on r_d value changing impedance (α)

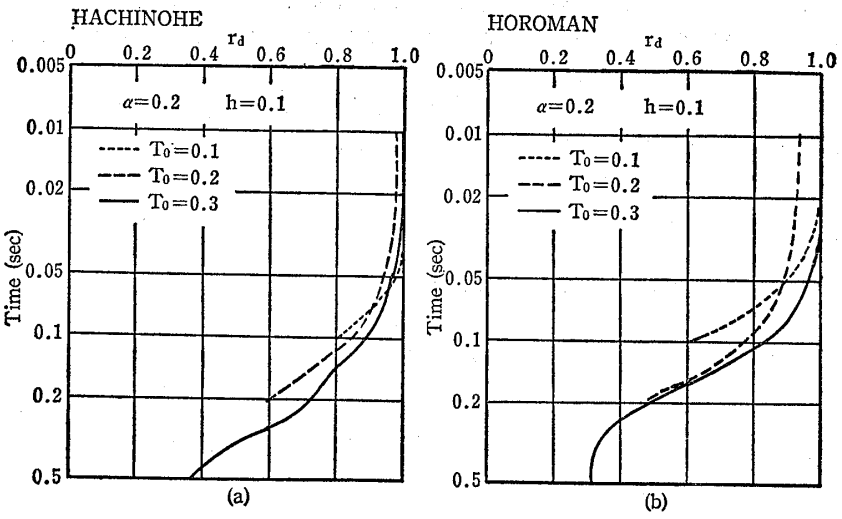

Fig. 14 Effect on r_d value changing travel time (T_0)

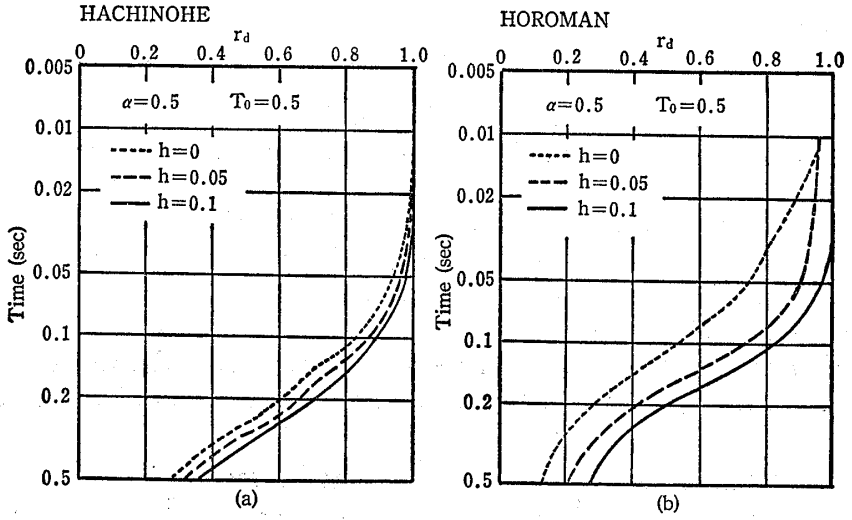

Fig. 15 Effect on r_d value changing damping factor (h)

waves were observed. However, no constant tendency in this change can be seen.

Figure 15 shows the effects of damping factor h. In this case, as h increases, there is a tendency for r_d to increase for all waveforms. This tendency is especially outstanding in the HOROMAN waves.

As we have seen in the above, of the three parameters considered, α, T_o and h, there is no marked influence on r_d values by α or T_o, while h does show an influence. Accordingly, we have calculated representative r_d distribution curves in relation to damping factor when $h=0$, 5% and 10%. Figure 16 shows the results of these calculations.

Figure 16 shows collectively the range of r_d distribution values calculated on the basis of previously conducted response analyses shown in Figure 11. Comparing these results, it can be seen that there is good correspondence between r_d distribution curves for damping factors of 5% and 10%.

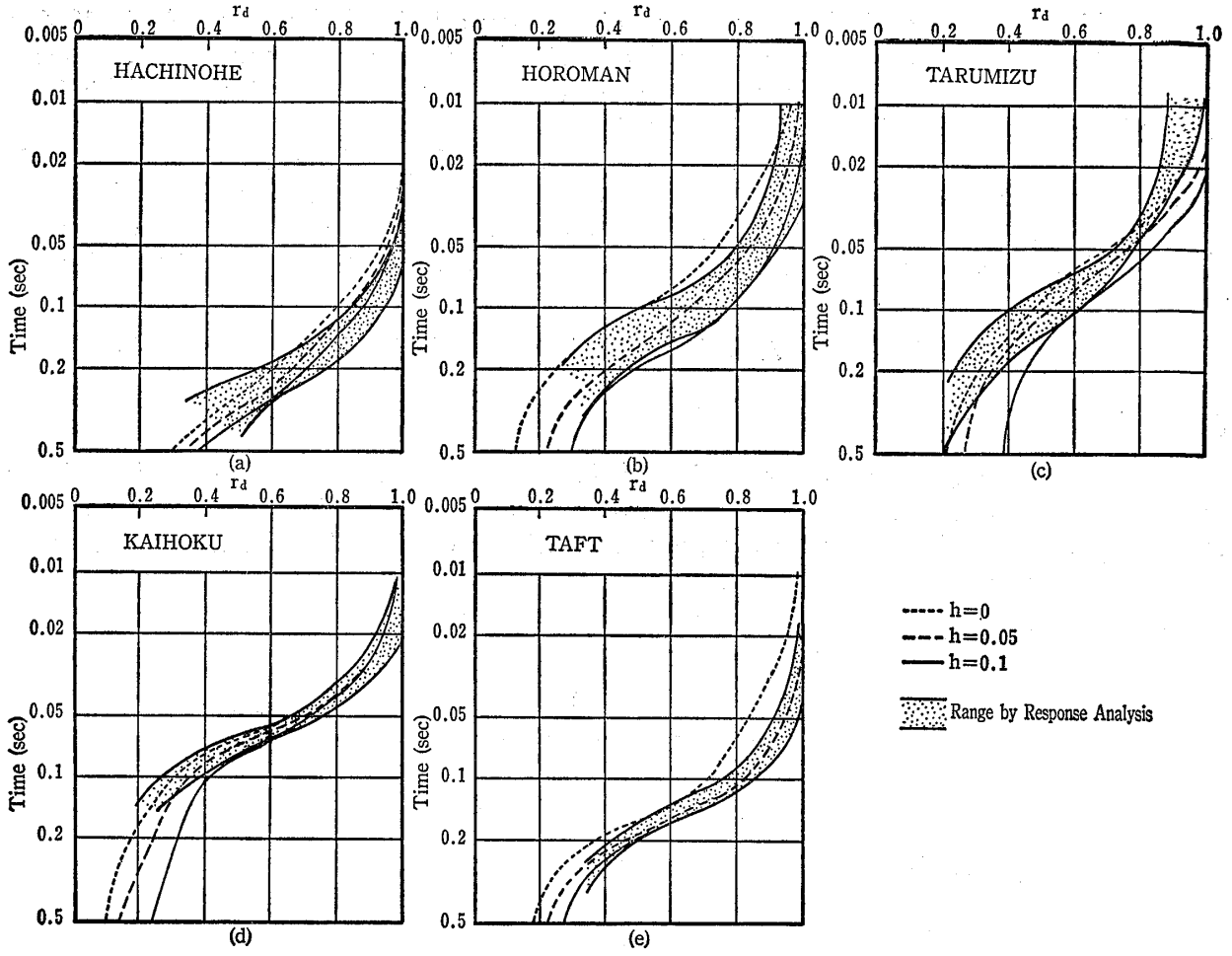

Fig. 16 r_d distribution for each wave

5.4 Effects of Damping Factor h

First, let us consider r_d from the standpoint of wave motion theory again. In the process of arriving at Formulas (6) and (7), a semi-infinite medium was hypothesized. For boundary conditions, it was given that the incidental waves are completely reflected from the surface as downward waves of the same amplitude. However, these conditions apply not only to our hypothetical semi-infinite medium, but also to any multilayered ground if we consider only the first layer. Consequently, Formulas (6) and (7) which assume a semi-infinite medium may be applied to the two-layer model of Section 5. 3. Furthermore, if we introduce amplitude v_0 not as amplitude of waves incidental to the base layer, but rather as the amplitude of response waves at the surface. When complex rigidity $G^*=G(1+2hi)$ is used in Formula (5), the following formulas, which also take viscosity into account, are derived:

$$r_d=\frac{1}{\omega T}\sqrt{\frac{1+h^2}{1}\{\cosh(2\omega Th)-\cos 2\omega T\}} \tag{8}$$

$$r_d=\frac{e^{\omega Th}}{2\omega T}\sqrt{1+h^2} \tag{9}$$

Formulas (8) and (9) correspond to Formulas (6) and (7) respectively.

Figure 17 shows single frequency r_d distribution calculated for when h=0, 10% and 20%. In this figure, y axis is normalized by multiplying frequency by travel time. As shown in the figure, as damping factor h increases, there is a tendency for r_d to increase. This is consistent with the above mentioned model calculations.

We may therefore conclude that in cases where a substantial number of response analysis results are not available, in order to determine generalized r_d distribution curves such as shown in Figure 11 (f), it is acceptable to use either the 5% or 10% damping time-related r_d distribution values for the two-layer model shown in Figure 16 to select a representative r_d distribution curve.

6 PROPOSAL FOR A NEW SIMPLIFIED EVALUATION METHOD

6.1 Evaluation Procedure

Below is a proposal for evaluation of shear stress which takes into consideration the dependency of S wave velocity (rigidity) on strain. Figure 18 summarizes the procedure.

(1) First, specify the constants for a ground model and calculate S wave travel time from the surface to the center of the first layer.

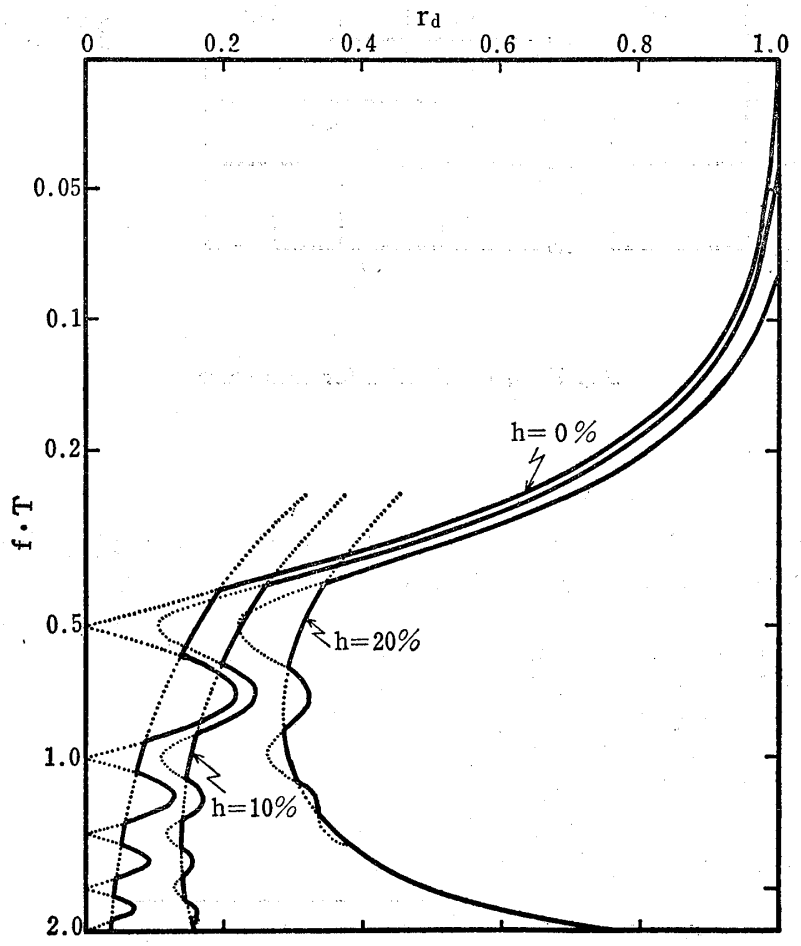

Fig. 17 Theoretical r_d distribution in semi-infinite media calculated in consideration of damping factor

(2) Pick out r_d value corresponding to travel time calculated above from the r_d curve for the specified wave form.

(3) Determine shear strain by dividing shear stress by rigidity.

(4) After substituting effective shear strain for the shear strain value obtained, use the strain dependence curve (Figure 20) to change S wave velocity so that it agrees with this value.

(5) Using the new S wave velocity, repeat steps (1) through (4) until relative error between strain value before and after the calculation process converges to within 10%.

(6) Once convergence is achieved in the first layer, go on to the second and the third layers, determining converged S wave velocity for each layer above the base layer.

(7) Using the pattern of S wave velocities thus obtained, calculate travel time to the desired depth. Then, using r_d value taken from the r_d distribution curve, determine shear strain.

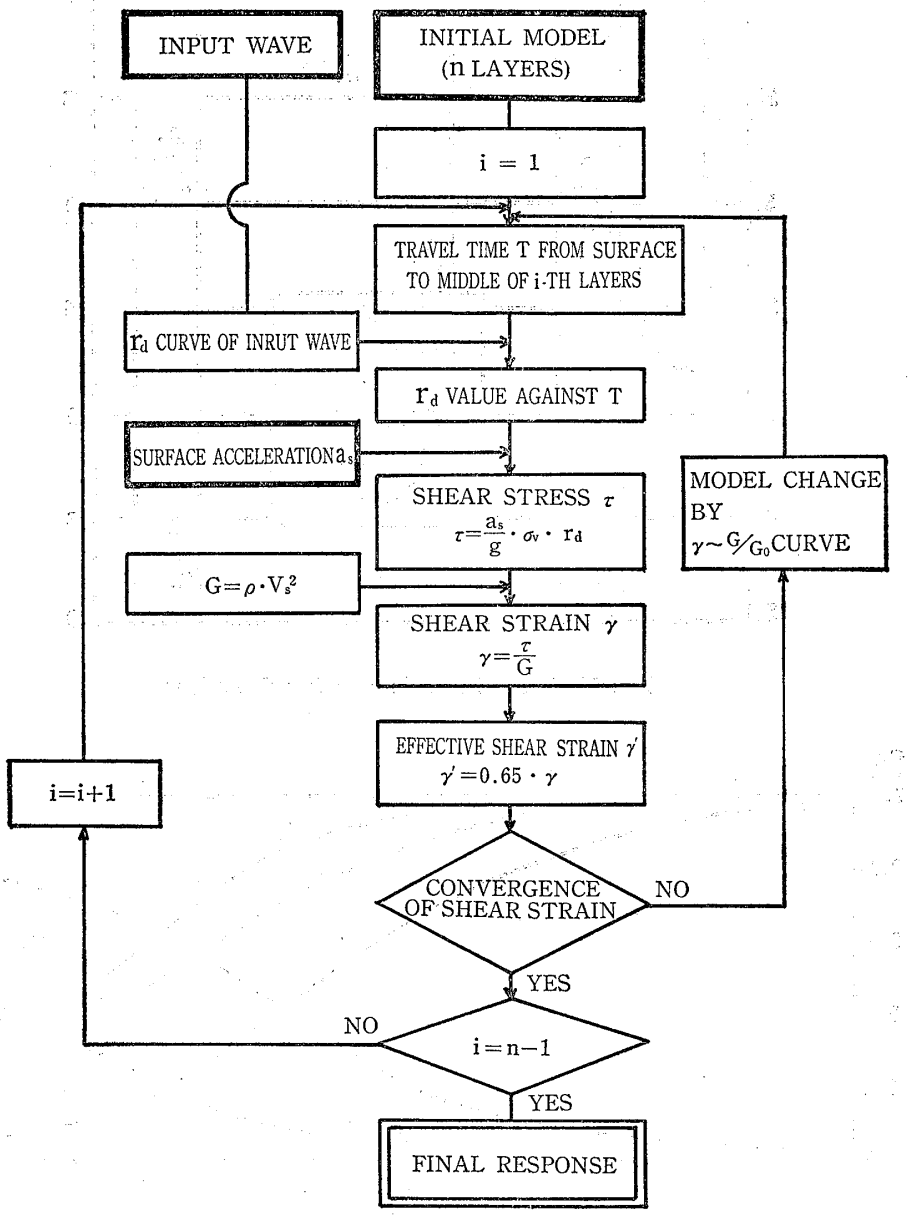

Fig. 18 Procedure of simplified method of evaluating shear stress during earthquake

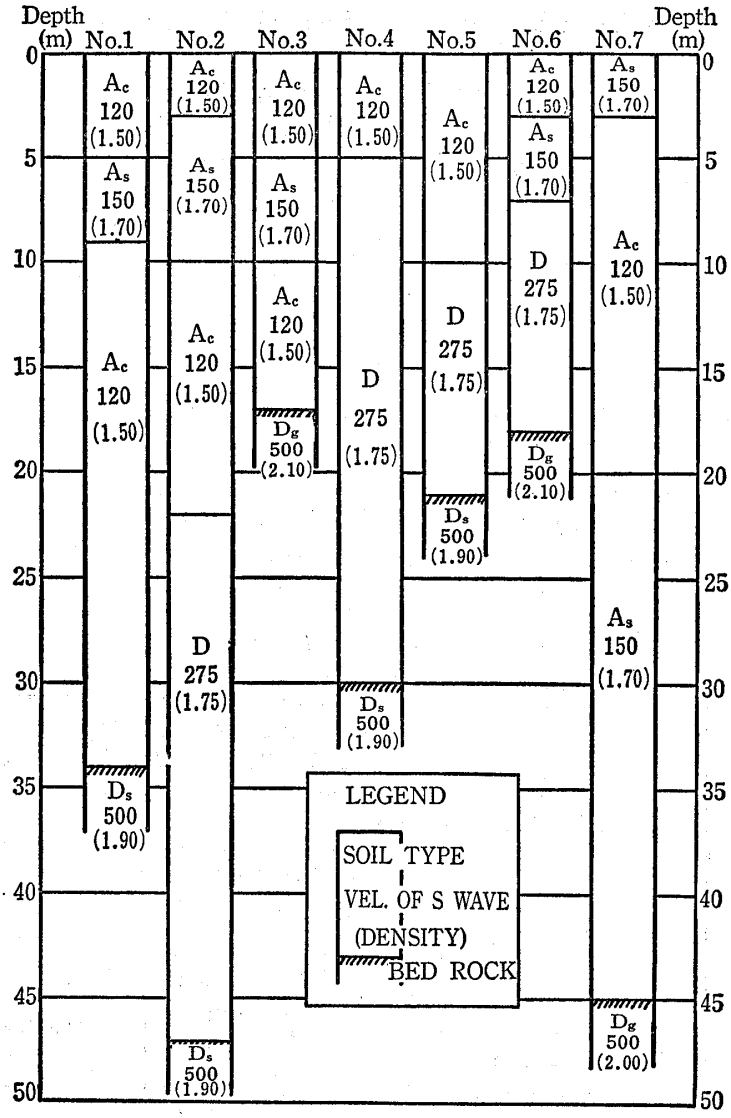

Fig. 19 Ground models used in calculations

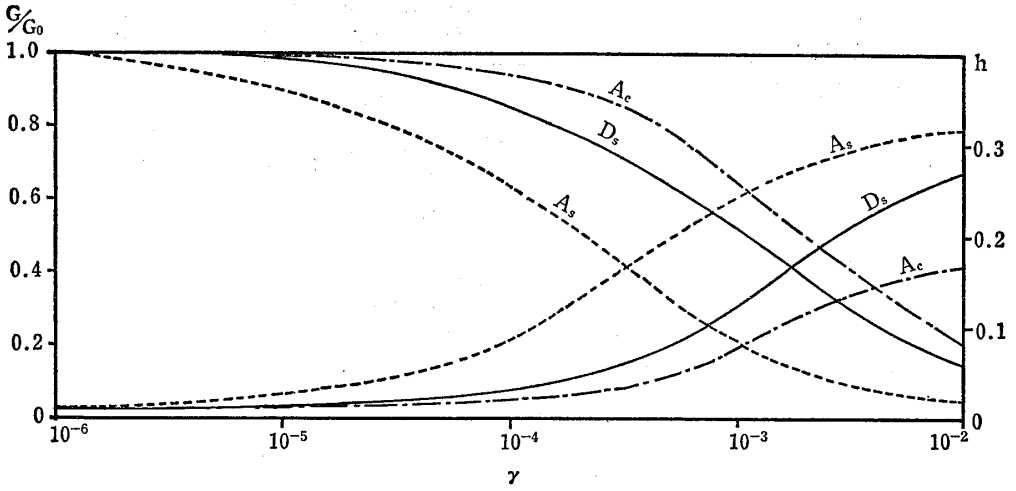

Fig. 20 Strain dependency curves of rigidity (G/G_0) and damping factor (h)

6.2 Example of Application of Evaluation Method

As shown in Figure 19, the authors carried out response analysis on 7 kinds of ground models by using HACHINOHE and KAIHOKU waveforms at incidental acceleration amplitudes of 100 gal. Then they compared these results to shear stress values computed on the basis of Seed's simplified formula. Here, the following three values obtained by each of these methods are compared:

(a) Time-related r_d distribution where the S wave velocity is reduced by strain, which is obtained by the procedure described in Section 6. 1.

(b) Time-related r_d distribution where the S wave velocity used is that used in the initial model.

(c) Depth-related r_d distribution. Here the value for r_d used is $1-0.015 \cdot z$. The strain dependence curve for rigidity and damping factor is shown in Figure 20.

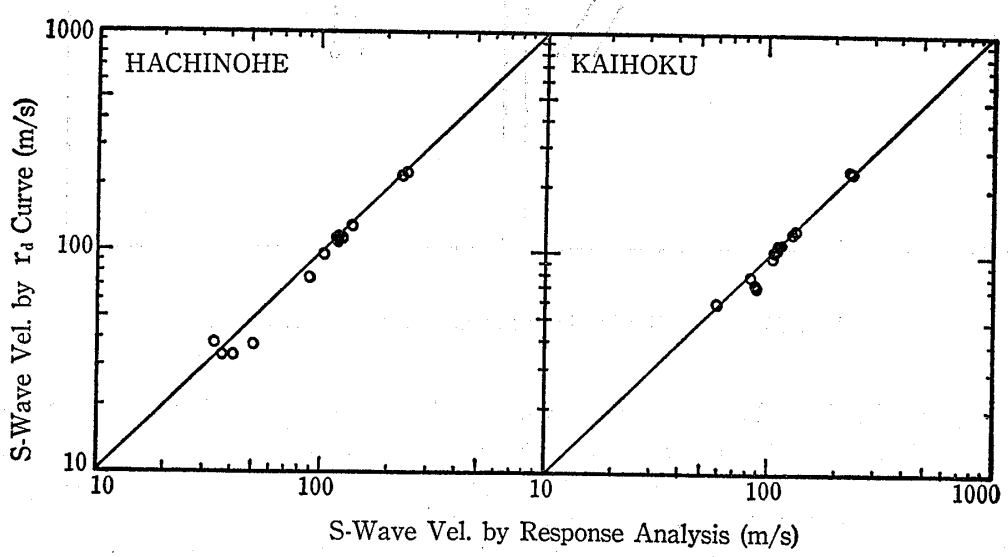

Fig. 21 Comparison of S wave velocities obtained by response analysis and simplified method (a)

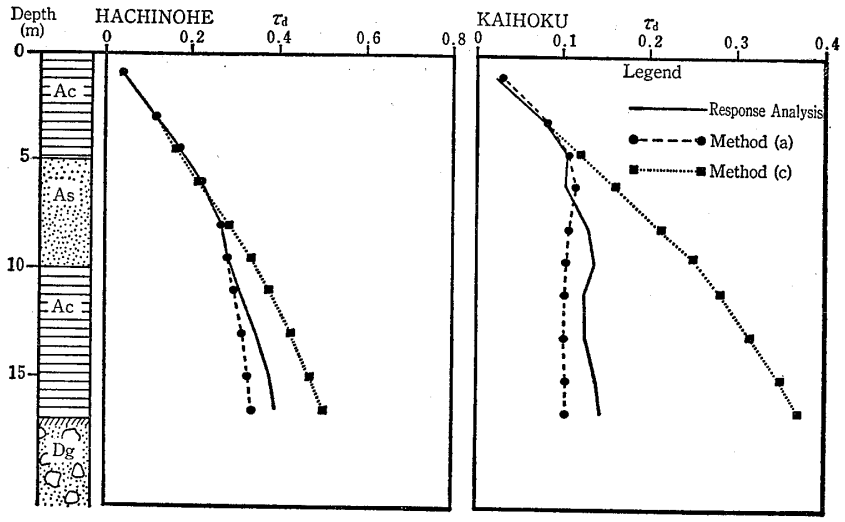

Fig. 22 Depth distribution of shear stress (model No. 3)

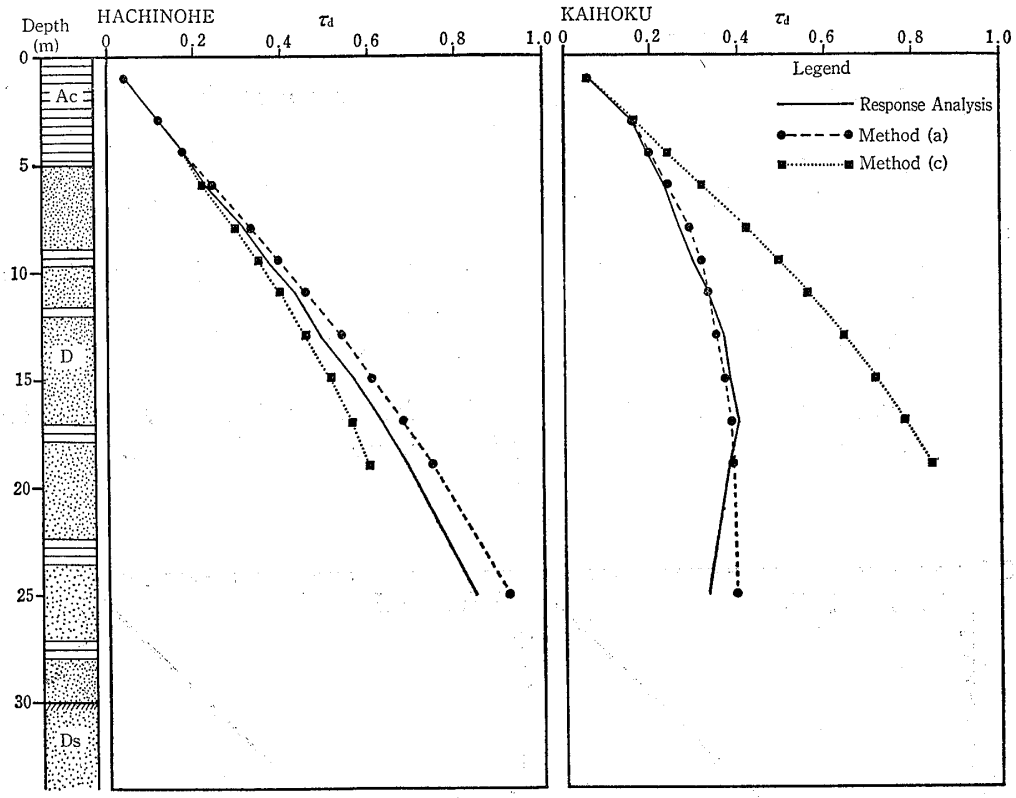

Fig. 23 Depth distribution of shear stress (model No. 4)

Before evaluating shear stress, S wave velocity values obtained by response analysis were compared with the results of the procedure described in Section 6. 1. This comparison is shown in Figure 21. The figure shows relatively good agreement between the two methods. Thus, the authors' proposal may be supposed to be valid.

Figures 22 and 23 are a comparison of values obtained through response analysis and methods (a) and (c) for shear stress depth distribution in two models selected from the above mentioned 7 models. For HACHINOHE input waves, little difference in values obtained by any of the methods results for either model. However, for KAIHOKU input waves, there is a great difference between results obtained by method (c) and the other methods for any model.

In Figures 24 and 25 the results of shear stress obtained from all 7 models is compared. In these figures, error is within a range of $\pm 25\%$. All results obtained by proposal (a) fall within this range, amounting to good agreement. With method (b), good agreement is shown, although these results are generally somewhat larger than actual values. With the old method (c) there are some areas of agreement, while in others, depending on the ground model, there are big differences.

In this way, using the authors' proposed time-related r_d distribution for corrected evaluation, the results obtained show good agreement in all ground conditions.

7 AFTERWORD

In this paper we have investigated the correction coefficient r_d in Seed's method for evaluating shear stress generated during earthquakes by response analysis. This investigation was based on the results of numerous response analyses carried out by the authors. We have pointed out that S wave travel time and incidental waveforms are basic factors influencing r_d

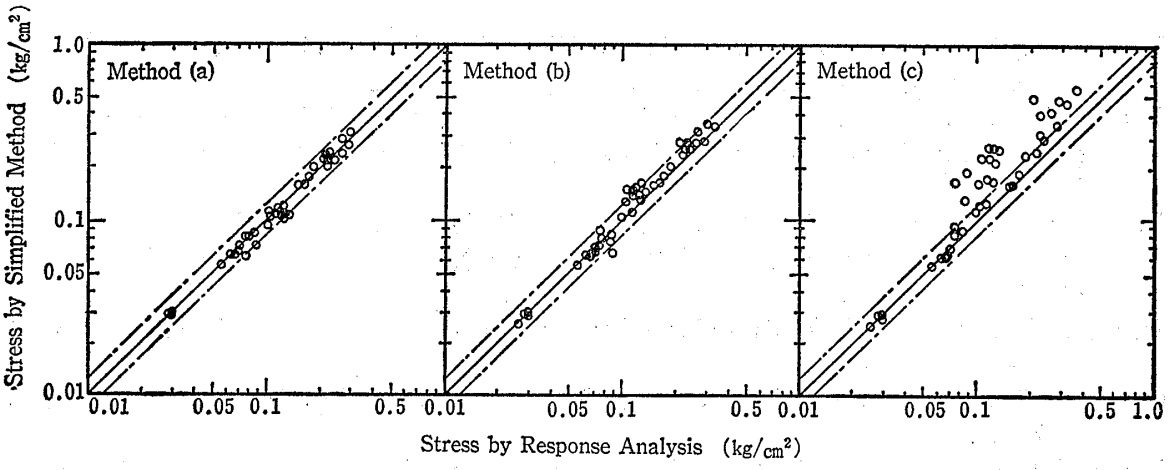

Fig. 24 Comparison of shear stress obtained by response analysis and various simplified method (input wave : HACHINOHE)

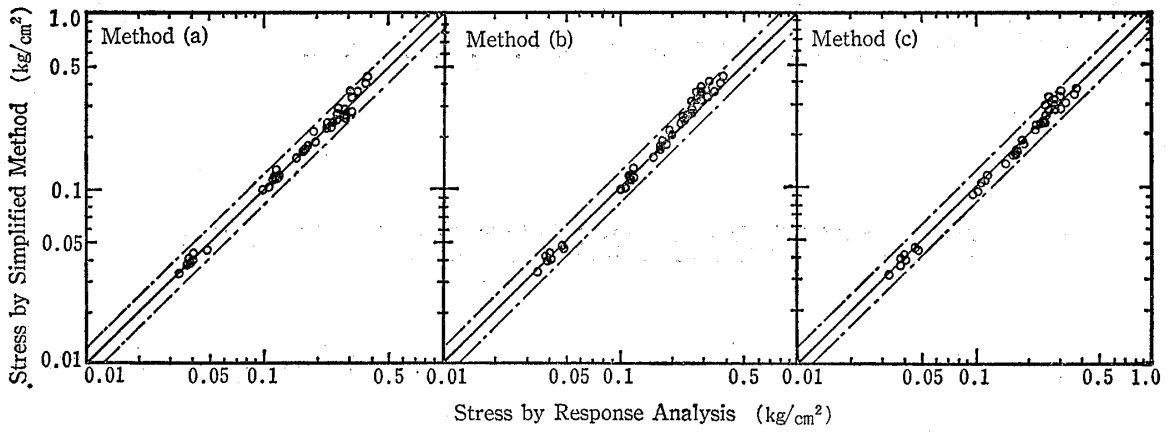

Fig. 25 Comparison of shear stress obtained by response analysis and various simplified method (input wave : KAIHOKU)

values. On the basis of this, we have proposed a time-related r_d curve. This time-related method is nothing more than the normalization of r_d values. If time-related r_d values are used, values more closely approximating actual shear stress will be obtained than with depth-related r_d values. Nevertheless, it cannot be denied that a certain amount of error is included. However, regardless of whether or not it was actually possible to refine this method further, even if this was feasible, the process of computation would become complex, and the advantages of having a simplified method would be lost. Our method uses a quasistatic concept, although it would be more accurate to regard it as a time history method.

In this way, the time-related r_d distribution method proposed by the authors may be described as a suitable method when considered from the standpoint of ease of use and accuracy of results obtained.

References

1. Seed, H. B. and I. M. Idriss (1971), "Simplified procedure for evaluating soil liquefaction potential", Proceedings of A. S. C. E. SM9.

2. Iwasaki, T., H. Tatsuoka and K. Tokita (1978), "Method on estimation of soil liquefaction" (in Japanese), Civil Engineering Journal, vol. 20, no. 4.
3. Kanemori, T., K. Tonouchi and T. Imai (1980), "Evaluation of shear stress in ground generated during earthquakes" (in Japanese), 35th Annual Meeting of Japan Society of Civil Engineers.
4. Tonouchi, K., T. Kanemori and M. Yamamoto (1981), "Evaluation of shear stress in ground generated during earthquakes (II)" (in Japanese), 8th Annual Meeting of Kantou Chapter of Civil Engineers.
5. Haskell, N. A. (1953), "The dispersion of surface waves on multilayered media", Bull. Seism. Soc. Amer., vol. 43.
6. California Institute of Technology (1969), "Strong motion earthquake accelerograms", E. E. R. L. 70-20.
7. Port and Harbor Research Institute (1969), "Strong motion earthquake records on the 1968 Tokachi-oki Earthquake and its aftershocks", Technical Note of the P. H. R. I. no. 80.
8. Public Works Research Institute (1978), "Strong motion acceleration records from Public Works in Japan (no. 2)", Technical Note of the P. W. R. I., vol. 32.
9. Public Works Research Institute (1978), "Strong motion acceleration records from Public Works in Japan (no. 3)", Technical Note of the P. W. R. I., vol. 34.

地中の地震時発生せん断応力の簡易評価法

今井常雄・殿内啓司・兼森　孝

概　要

構造物の耐震設計や砂質地盤の液状化の可能性の検討にあたっては，加速度・速度あるいは変位といった各種振巾の予測と同様，地中の地震時発生せん断応力の評価もまた重要である。一般に，これらを得るために，波動論に基づく方法，集中質量法あるいは有限要素法等を用いた地盤の地震時応答解析が行なわれる。また一方では，こういった複雑な方法とは別に，Seed の提案に代表される簡易な地震時発生せん断応力の評価法もよく用いられている。この方法は地盤内の単位土柱を剛体としてのベースシャをもとに，実際には剛体でないことによる違いを補正するための補正係数 r_d を用いて評価するものである。この補正係数 r_d については Seed のほか，岩崎・他によっても提案されているが，さほど詳細な検討がなされていないのが実情である。

本報告では，まず，この補正係数 r_d について，筆者らがこれまで数多く実施してきた波動論に基づく方法を用いての応答計算結果をもとに，種々の検討を行なった。そして，その結果をふまえて地震時発生せん断応力の簡易評価法を提案し，併せてこの方法による具体的評価例を示した。

従来提案の r_d は Fig. 2 に示すように，深さの関数として与えられている。しかしながら，応答計算結果から求まる r_d を同様に整理してみると，その分布曲線は，Fig. 6 に示すように，r_d は極めて広い範囲に分布しており，既往の提案のように各深度で一定なものではなく，入力条件や地盤条件等に支配されて変動するものであることが明らかとなった。

種々の検討の結果，地盤モデルによる r_d 分布の違いは，地盤のS波速度構造に着目して，r_d を走時の関数として表現することによって規準化できた。そこで，Fig. 11 (f) に示す波形別の標準曲線とこれを用いてのせん断応力評価法を提案した (Fig. 18)。ここに提案の方法を用いて実際のモデルで評価した結果 (Fig. 22～25) より，この方法は詳細な応答解析結果を充分に説明できる実用評価法といえよう。